引用格式：WANG Xuquan, HUANG Songlei, KE Pengyu, et al. Improvement of LVF-based NIR Spectral Sensor on Both Spatial and Time Domains[J]. Acta Photonica Sinica, 2021, 50(4):0430001
王绪泉,黄松垒,柯鹏瑜,等.集成滤光片型近红外光谱组件的时空域性能改善研究[J].光子学报,2021,50(4):0430001

集成滤光片型近红外光谱组件的时空域性能改善研究

王绪泉[1,2,3],黄松垒[1,2],柯鹏瑜[1,2,3],刘梦璇[1,2],赵振力[1,2],方家熊[1,2]
(1 中国科学院上海技术物理研究所 传感技术联合国家重点实验室,上海 200083)
(2 中国科学院上海技术物理研究所 中国科学院红外成像材料与器件重点实验室,上海 200083)
(3 中国科学院大学,北京 100049)

摘 要:提出针对线性渐变滤光片型近红外光谱组件的时空域性能改善方法,并通过研制微型化512×2元InGaAs光谱组件,结合多帧数据融合算法完成了实验验证。光谱通道采用基于多次测量的两列相邻光敏元动态组合实现,相比单个大光敏元作为光谱通道,可以改善探测器盲元引起的不良影响。波长标定和测试结果表明,该光谱组件在线性渐变滤光片的分辨率限制下,可以有效减小相邻光谱通道间的波长间隔。

关键词:铟镓砷;光谱组件;线性渐变滤光片;波长标定;近红外
中图分类号:TN219 **文献标识码**:A **doi**:10.3788/gzxb20215004.0430001

Improvement of LVF-based NIR Spectral Sensor on Both Spatial and Time Domains

WANG Xuquan[1,2,3], HUANG Songlei[1,2], KE Pengyu[1,2,3], LIU Mengxuan[1,2], ZHAO Zhenli[1,2], FANG Jiaxiong[1,2]
(1 *State Key Laboratories of Transducer Technology, Shanghai Institute of Technical Physics, Chinese Academy of Sciences, Shanghai* 200083, *China*)
(2 *Key Laboratory of Infrared Imaging Materials and Detectors, Shanghai Institute of Technical Physics, Chinese Academy of Sciences, Shanghai* 200083, *China*)
(3 *University of Chinese Academy of Sciences, Beijing* 100049, *China*)

Abstract: The method to improve performance of Linear Variable Filter (LVF) based spectrometers is proposed and validated. By this means, a compact 512×2 InGaAs spectral sensor with dynamic data fusion on both spatial and time domains is developed. In the spectral sensor, spectral channel is not a single pixel but a group of neighboring pixels with multi-frame measurements. The data from two pixel arrays are multiplexed to compensate possible sensor defects such as blind pixels. The wavelength calibration and experimental results show that the proposed methods can significantly reduce the wavelength spacing

Foundation item: National Natural Science Foundation of China(No.61376052), the Open Project Program of the State Key Laboratories of Transducer Technology of China (No.SKT1907), the Open Project Program of the State Key Laboratories of Infrared Physics of China (No.M201901)
First author: WANG Xuquan (1989—), male, research associate, Ph. D. candidate. mainly focuses on near-infrared sensor and integrated circuit design. Email: wangxq@mail.sitp.ac.cn
Supervisor(Contact author): HUANG Songlei (1984—), male, associate research fellow, Ph.D. degree, mainly focuses on design of infrared read out integrated circuit. Email: huangsl@mail.sitp.ac.cn
Received: Dec.9,2020; **Accepted**: Jan.28,2021

between spectral channels with the optical resolution limit of LVF.

Key words: InGaAs; Spectral sensor; Linear variable filter; Wavelength calibration; Near-infrared
OCIS Codes: 300.6190; 040.3060; 040.5160; 130.7408; 230.7408

0 Introduction

The commercial application of spectral analysis is an important driving force to the miniaturization of Near Infrared (NIR) instruments[1-5]. Several techniques are adopted in micro-spectrometer considering the cost and system complexity. Fourier Transform Infrared (FTIR) spectrometer is not widely applied in portable applications because of structural complexity and unfixed components. Grating and Micro-Electromechanical Systems (MEMS) are the general selection for compact spectral instruments, but the size and cost were still not good enough[1]. Acousto-Optic Tunable Filter (AOTF) spectrometer has been applied to imaging spectrometers with the advantages of size, but not commonly used in NIR spectroscopy because of poor uniformity and high price[1]. The spectrometer based on Linear Variable Filter (LVF) and detector array has an extremely compact and rugged structure without unfixed parts[6-10]. Compared to the optical grating, the resolution of LVF is relatively low at present. It is about 10～20 nm in the range of 900～1 700 nm[11]. However, considering the advantages of LVF in cost, flux, size and uniformity, LVF-based spectrometer is still an ideal choice for miniaturized and portable applications.

Due to the maturity of manufacturing process, the spectrometer based on CMOS sensors is more common in research and utilization[12-13]. InGaAs detectors own the advantages of fast response and high sensitivity in Short-Wave Infrared (SWIR) waveband[14]. The spectrometer with LVF and InGaAs Focal Plane Array (FPA) has been applied in many portable analysis applications[6-10]. Adopting this structure, a InGaAs spectral sensor with 256×1 pixels and 50 μm pitch was studied in our previous work[15-16]. In theory, for an ideal LVF with fixed size, a larger detector array with decreasing pixel pitch could bring more spectral channels. However, the resolution of LVF-based spectrometers is generally limited by the performance of LVF at present[17]. A performance-limited LVF and a larger FPA cause serious spectral crosstalk between neighboring channels, which cannot improve the resolution of spectrometer effectively. Moreover, the single-column InGaAs FPA was used in most of previous studies[15-16]. The spectral curve might be severely affected by blind pixels.

In this study, a spectral sensor integrating LVF and a 512×2 InGaAs FPA with the pitch of 25 μm is investigated. Two pixel arrays are placed in parallel in this spectral sensor, which is different from our earlier research. Spectral channels are defined as the combination of several contiguous pixels and separated by unused pixels, which can solve the problem of spectral crosstalk effectively. The pixel number in each spectral channel is calculated based on the performance of LVF. A transformation method of spectral channels is proposed to reduce the wavelength spacing between spectral channels by changing the combinations of pixels dynamically. With multi-frame measurements and data fusion algorithm, more useful spectral signature can be obtained with the limited resolution of LVF. On one hand, the combination of pixels can significantly reduce the influence of blind pixels on the spectral curve. On the other hand, a higher Signal-to-Noise Ratio (SNR) can be obtained by signal accumulation with the same integral time.

Herein, the structure of spectral sensor with a custom-built LVF is discussed in detail firstly. The performance characterization and wavelength calibration are conducted to show the spectral crosstalk degree between neighboring pixels. As the improved solutions, performance improvement methods with dynamic data fusion on both spatial and time domains are proposed and validated. The validation results show that the proposed methods can significantly reduce the wavelength spacing between spectral channels with the optical resolution limit of LVF.

1 Methodology

1.1 Architecture of Spectral Sensor

The LVF is a wedge-shaped and dielectric thin-film Fabry-Perot bandpass filter[18]. As a result of the varying film thickness, the wavelength transmitted through the filter varies linearly in the direction of the wedge[19]. The basic performance of LVF was characterized in order to confirm the optimal coupling and

assembly structure. The Nicolet 6 700 FTIR spectrometer, a 20 μm slit, and a precision positioning micro-displacement platform were used in this experiment. The LVF and slit were fixed on the micro-displacement platform. The function of the slit is to limit the region of LVF. The slit width of 20 μm is close to the pixel pitch of FPA, so the result is instructive in the subsequent design. The transmittance of LVF was observed from side to side with a step of 0.5 mm. The results are shown in Fig. 1. The effective size of LVF is 13 mm and the wavelength range is from 900 nm to 1 700 nm. The peak transmittance is between 25% and 75% for the incident light. The transmittance function of LVF is very consistent with the characteristics of Cauchy-Lorentz distribution. The fitting curve is shown in Fig. 1 with the fitting formula as follows

$$y = y_0 + \frac{2A}{\pi} \cdot \frac{w}{4(x - x_c)^2 + w^2} \tag{1}$$

where, x_c is the peak wavelength, w is the Full Width at Half Maximum (FWHM), A is the area, and y_0 is the offset on Y-axis which is closed to zero in this formula. The peak wavelengths have a good linearity, indicating that the LVF has a good consistency in full passband. The FWHM distributes from 14 nm to 18 nm except the edge of filter, which is between 1% and 1.5% of the peak wavelength.

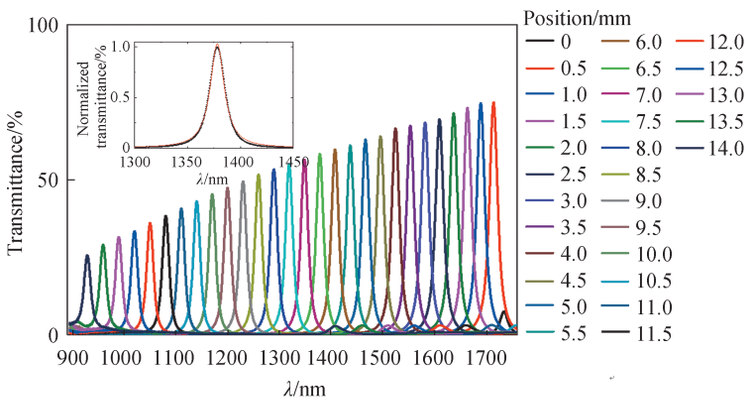

Fig.1 The transmittances of LVF

The Linear Dispersion Coefficient (LDC) of LVF can be calculated by

$$\mathrm{LDC} = \frac{\Delta\lambda}{\Delta L} = 61.5\ \mathrm{nm/mm} \tag{2}$$

The InGaAs FPA was designed based on the above parameters. The minimum FWHM of 14 nm was selected for calculation in order to get an appropriate design margin. Thus, the length of LVF corresponding to the minimum FWHM is

$$L_{\min} = \frac{\mathrm{FWHM}}{\mathrm{LDC}} = 228\ \mu\mathrm{m} \tag{3}$$

This value is more than four times of the pitch in our previous research, which confirms our claim that the resolution of LVF is the key restriction of this kind spectrometers. Herein, a 512×2 InGaAs FPA with pixel size of 25 μm×25 μm was used to match with the LVF. Two pixel arrays were placed in parallel with a distance of 25 μm. The pixel size is about 1/10 of Lmin and the peak wavelength spacing between pixels is much less than FWHM. The spectral responses of neighboring pixels are exceedingly similar and highly overlapped. Thereby, pixels can be regarded as ideal points under the coverage of LVF.

A smaller space between LVF and FPA can decrease the spectral crosstalk and improve the resolution of spectral sensor. The assembly structure of spectral sensor is shown in Fig. 2 (a). The InGaAs chip and its readout circuit (ROIC) were interconnected with flip chip technology. The LVF was fixed behind the diaphragm and then flipped over the FPA. The height between FPA and diaphragm is 0.5 mm, equal to the thickness of LVF. In order to reserve an appropriate design margin, a U-shape groove with a depth of 0.1 mm was designed at the bottom of the diaphragm. Therefore, the distance between LVF and FPA is about 0.1 mm, which is a relatively reasonable size. The spectral sensor was packaged in a metal shell as shown in Fig. 2 (b). The specification of this spectral sensor is shown in Table 1.

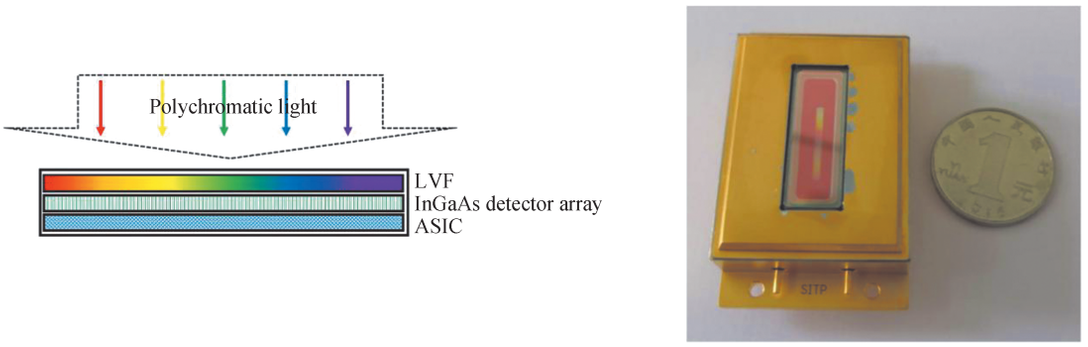

(a) The structure of 512×2 InGaAs spectral sensor

(b) The picture of 512×2 InGaAs spectral sensor

Fig. 2 512×2 InGaAs spectral sensor

Table 1 The specification of spectral sensor

Parameter	Typical value
Spectral range	900 nm to 1 700 nm
Number of pixels	512×2
Pixel size	25 μm×25 μm
Dimensions	55 mm (L)×33 mm (W)×13 mm (H)
Weight	<80 g
Power requirement	< 25 mA@3.3 V
Operating temperature	−20~60 ℃

1.2 Measurement and Calibration

The basic performance of spectral sensor was measured as the validation of design and analysis. The structure of experimental platform is shown in Fig.3, including the monochromator iHR550 (HORIBA, Japan) with a tungsten halogen lamp as light source and an optical collimator, the data generator DTG5078 (Tektronix, USA), the modular power system N6700B (Agilent Technologies, USA), the SR560 low-noise preamplifier (SRS, USA), an NI data acquisition (DAQ) card embed in the industrial computer with data processing software.

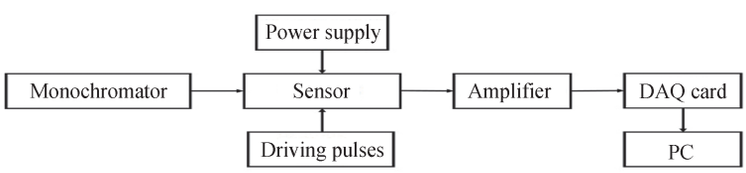

Fig. 3 The structure of experimental platform

The grating of the monochromator was set to 950 lines/mm. Both the inlet slit and the outlet slit were 4 mm. The monochromatic lights from 900 nm to 1 700 nm were generated with a wavelength step of 1 nm. The integration time of spectral sensor was set to 2 ms. The wavelength calibration is highly dependent on the relative spectral responses of all pixels. The general FPA DAQ system was used to collect the relative spectral responses to monochromatic lights. With fitting algorithm, the peak wavelength and FWHM of each pixel can be calculated from the relative spectral responses. Accordingly, the definition of spectral channels and the result of wavelength calibration can be concluded to match with the specifications of LVF. Finally, the NIR wavelength standard reference material SRM-2035a (NIST, USA) was used as validation of the wavelength calibration[20].

2 Results and discussions

The detailed relative spectral responses of pixel No. 299 to pixel No. 303 are shown in Fig. 4, demonstrating that the neighboring curves overlap seriously. This is coincident with our previous theoretical

analysis that the resolution of this kind spectrometer is limited by the performance of LVF. Therefore, it is no longer effective to improve the resolution by simply reducing the pixel size in this condition.

As shown in Fig.5, the peak wavelength and FWHM of each pixel were calculated from the above curves by Cauchy Lorentz fitting. The results show that the peak wavelength of each pixel has a good linearity, which is consistent with the performance of LVF. The average value of wavelength interval is 1.46 nm, slightly less than the predicted value of 1.56 nm. The reason is probably that the short-wave of LVF does not start at 900 nm strictly, but it is slightly larger. After correction, the calculated value is coincident with the experimental value. The FWHM increases slowly as the increase of peak wavelength. Most values are between 12 nm and 16 nm except serval pixels under the edge of LVF, which is also coincident with previous analysis. Since the wavelength spacing is about 1/10 of FWHM, several neighboring pixels are grouped as spectral channel for calibration.

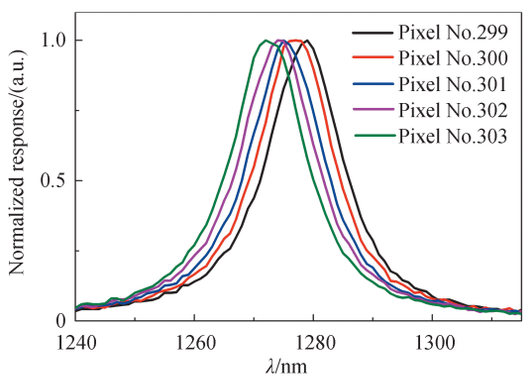

Fig. 4 Relative spectral response of pixels

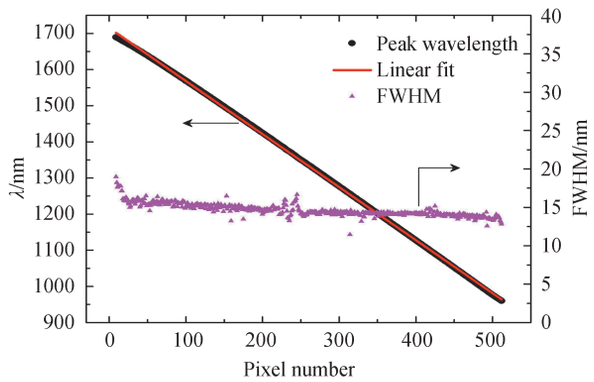

Fig. 5 The peak wavelength and FWHM of each pixel

The spectral channels are defined in accordance with the following criterions. According to theoretical calculation, the length corresponding to the minimum FWHM of LVF is 228 μm. In order to make full use of LVF, at least two spectral channels are deployed within this length. In addition, a suitable distance should be reserved between spectral channels so that the overlap of spectral curves is acceptable. Considering the size of pixel, three neighboring pixels are finally grouped as a spectral channel. The calibration wavelength of the middle pixel is used as the wavelength of spectral channel. Two pixels are reserved as spacing between neighboring spectral channels. In this way, more than 100 spectral channels can be acquired with an equivalent width of 75 μm and 50 μm space. Six neighboring channels between pixel No. 290 and pixel No. 317 are selected as example in Fig.6. The wavelength spacing between channels is 7.4 nm, which is about half of the FWHM. The normalized curves show that the crosstalk of neighboring channels has been remarkably reduced. The crossover point of neighboring spectral curves is about 80% of the peak, which roughly meets the Rayleigh criterion. The experimental results prove that this group method of spectral channels is effective and feasible.

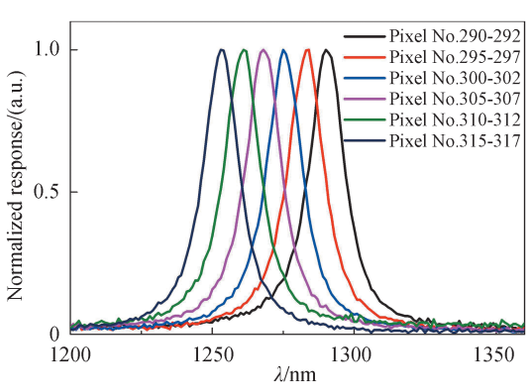

Fig. 6 Normalized spectral response of spectral channels

Based on the structure of spectral sensor and calibration results, a dynamic data fusion method is proposed to extract more spectral information. The implementation approach is that more than one frame spectral data were measured under the same condition. Different frame adopted different pixel combination in data processing. The pixel groups of spectral channel were shifted in multi-frame measurement to achieve a tiny step of wavelength. As shown in Fig.7, the data fusion of multi frames is realized through the shift of spectral channel. In this way, the wavelength step can be as small as the wavelength spacing of pixels, which is about 1.5 nm.

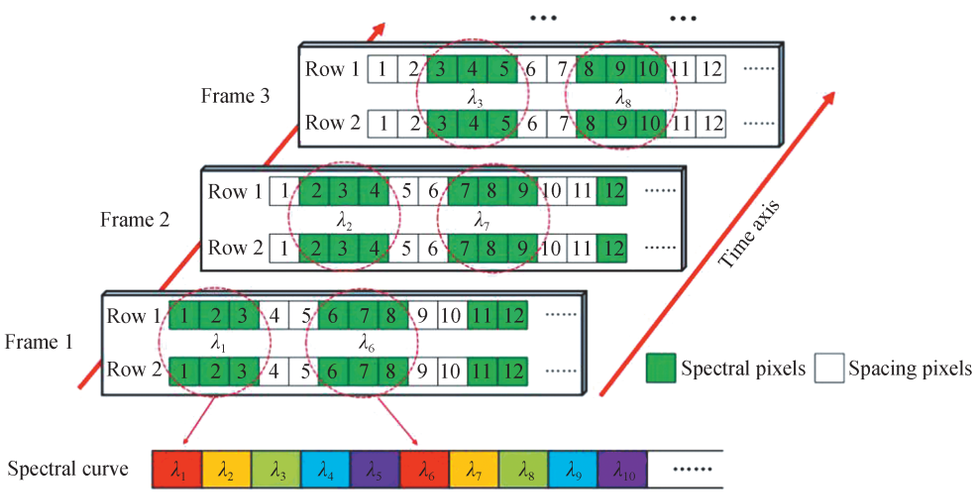

Fig. 7 The shift method of spectral channels

Finally, the absorbance of SRM2035a was measured using the above methods. The absorption curve is shown in Fig.8. The six absorption peaks in 900～1 700 nm are fitted, and the results are shown in Table 2. The experimental results show that the data fusion of multi-frame is beneficial to improve the fitting accuracy of absorbance peak compared with the conventional group method. The reason is that the spectral curve with data fusion contains more effective data points in the same spectral range. The effect is more significant especially in the fitting of small spectral peaks, such as peak 1 and peak 3.

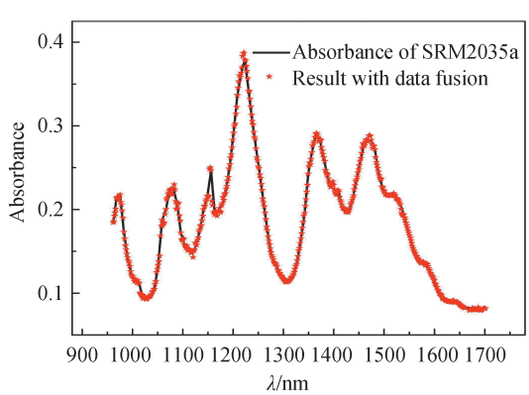

Fig. 8 The absorbance of SRM2035a with data fusion

Table 2 The absorption peaks of SRM2035a

Absorbance	Standard/nm	Offset without data fusion/nm	Offset with data fusion/nm
Peak 1	975.8 ± 0.1	+4.4	+2.8
Peak 1	1 075.6 ± 0.1	−3.0	−0.6
Peak 1	1 151.5 ± 0.1	+2.8	−1.7
Peak 1	1 222.2 ± 0.2	+0.9	+0.9
Peak 1	1 366.8 ± 0.1	−0.5	0
Peak 1	1 469.1 ± 0.2	+1.0	+0.4

3 Conclusions

In summary, a compact short-wave infrared InGaAs spectral sensor with dynamic data fusion on both spatial and time domains is developed. A 512×2 InGaAs FPA with the pixel size of 25μm×25μm and a LVF are integrated in the spectral sensor. In order to decrease the crosstalk, the spectral channel is defined as the combination of several neighboring pixels. A dynamic data fusion method of multi-frame measurement is also proposed. Different combination modes of spectral channels are applied in multiple measurements to extract more spectral information under the resolution limit of LVF. The wavelength calibration and experimental results show that the proposed data fusion method can significantly reduce the wavelength spacing of spectral channels. In addition, the combination of multiple pixels can decrease the negative influence of blind pixels and improve the SNR of spectrometer. In order to reflect the advantages of this sensor and data fusion method in spectral analysis, it is necessary to further study the optimized analysis model and algorithm.

References

[1] PASQUINI C. Near infrared spectroscopy: A mature analytical technique with new perspectives -A review[J]. Analytica Chimica Acta, 2018, 1026: 8-36.

[2] MA Xiao, ZOU Jun, LI Wenhuan, et al. Miniature spectrometer based on a Fourier transform spectrometer chip and a commercial photodetector array[J]. Chinese Optics Letters, 2019, 17(12): 123001.

[3] FRIEDRICH D, HULSE C, GUNTEN M, et al. Miniature near-infrared spectrometer for point-of-use chemical analysis [J]. SPIE, 2014, 8992: 899203.

[4] O'BRIEN N, HULSE C, FRIEDRICH D, et al. Miniature Near-Infrared (NIR) spectrometer engine for handheld applications[C]. SPIE, 2012, 8374: 837404.

[5] MARÍN D, PAZ P, GUERRERO J, et al. Miniature handheld NIR sensor for the on-site non-destructive assessment of post-harvest quality and refrigerated storage behavior in plums[J]. Journal of Food Engineering, 2010, 99: 294-302.

[6] SCHMIDT O, KIESEl P, BASSLER M. Performance of chip-size wavelength detectors[J]. Optics Express, 2007, 15 (15): 9701.

[7] SAXE S, SUN L, SMITH V, et al. Advances in miniaturized spectral sensors[C]. SPIE, 2018, 10657: 106570B.

[8] TIBÉRINI L, LEMARQUIS F, LEQUIME M. Masking mechanisms applied to thin-film coatings for the manufacturing of linear variable filters for two-dimensional array detectors[J]. Applied Optics, 2008, 47(30): 5706-5714.

[9] ZHANG Shaoda, WU Bin, XU Binbin, et al. Mixed-gas CH4/CO2/CO detection based on linear variable optical filter and thermopile detector array[J]. Nanoscale Research Letters, 2019, 14: 348.

[10] SCHMIDT O, KIESEL P, MOHTA S, et al. Resolving pm wavelength shifts in optical sensing[J]. Applied Physics B, 2007, 86: 593-600.

[11] CHU Xiaoli, Handbook of near infrared spectroscopy[M]. Beijing: China Machine Press, 2016.

[12] BLAIN P, NINANE N, MOREAU V, et al. Small facility for linear variable filter characterization[C]. SPIE, 2014, 10563: 1056357.

[13] FAN Shuxiang, WANG Qingyan, TIAN Xi, et al. Non-destructive evaluation of soluble solids content of apples using a developed portable Vis/NIR device[J]. Biosystems Engineering, 2020, 193: 138-148.

[14] LI Xue, GONG Haimei, FANG Jiaxiong, et al. The development of InGaAs short wavelength infrared focal plane arrays with high performance[J]. Infrared Physics & Technology, 2017, 80: 112-119.

[15] WANG Xuquan, HUANG Songlei, YU Yuehua, et al. Integrated linear variable filter / InGaAs focal plane array spectral micro-module and its wavelength calibration[J]. Acta Photonica Sinica, 2018, 47(5): 0530001.

[16] WANG Xuquan, HUANG Songlei, YU Yuehua, et al. A compact long-wavelength near-infrared IOT node and its performance experiments[J]. Journal of Infrared and Millimeter Waves, 2018, 37(01): 42-46.

[17] WIESENT B, DORIGO F, KOCH A. Limits of IR-spectrometers based on linear variable filters and detector arrays [C]. SPIE, 2010, 7767: 77670L.

[18] SHENG Bin, CHEN Peng, TAO Chunxian, et al. Linear variable filters fabricated by ion beam etching with triangle-shaped mask and normal film coating technique[J]. Chinese Optics Letters, 2015, 13(12): 122301.

[19] WANG Shifeng, YUAN Yan, SU Lijuan, et al. Measurement of the spectral characteristic parameters of linear variable filters[J]. Acta Photonica Sinica, 2017, 46(11): 1112002.

[20] DUEWER D, CHOQUETTE S, O'NEAl L, et al. Rare-earth glass reference materials for near-infrared spectrometry: sources of x-axis location variability[J]. Analytica Chimica Acta, 2017, 490: 85.